Liquid Crystals
Publication details, including instructions for authors and subscription information:
http://www.informaworld.com/smpp/title~content=t713926090

Textured deformations in liquid crystal elastomers

J. S. Biggins[a]
[a] Cavendish Laboratory, University of Cambridge, Cambridge, UK

First published on: 07 July 2009

To cite this Article Biggins, J. S.(2009) 'Textured deformations in liquid crystal elastomers', Liquid Crystals, 36: 10, 1139 — 1156, First published on: 07 July 2009 (iFirst)
To link to this Article: DOI: 10.1080/02678290902879224
URL: http://dx.doi.org/10.1080/02678290902879224

Liquid Crystals,
Vol. 36, Nos. 10–11, October–November 2009, 1139–1156

Taylor & Francis
Taylor & Francis Group

INVITED ARTICLE

Textured deformations in liquid crystal elastomers

J.S. Biggins*

Cavendish Laboratory, University of Cambridge, 19 JJ Thomson Avenue, Cambridge CB3 0HE, UK

(Received 12 February 2009; final form 9 March 2009)

Liquid crystal elastomers exhibit very rich elastic behaviour because they couple elastic fields and mobile liquid crystal order. One striking phenomenon is the formation of textured deformations: a homogenous elastomer sometimes responds to a macroscopically homogenous imposed strain by forming a spatially fine mixture of very different deformations (a texture) that average to the imposed strain. This occurs because some large strains can be accommodated by rotation of the liquid crystal order, so they cost little energy to impose, while other equally large (or smaller) strains cannot and hence are energetically expensive. If one of these latter strains is imposed macroscopically, the elastomer's energy is lowered if it can form a fine mixture of larger but lower energy strains that average to the imposed deformation. Great progress has been made in understanding this behaviour over the last 10 years. Here, we review the key theoretical ideas and highlight several predicted textures which merit experimental attention. This review assumes little prior knowledge of elasticity or liquid crystal elastomers so hopefully it will be accessible to both non-elasticians and elasticians from other fields, notably the study of martensite which is a highly analogous system but with small strains and discrete broken symmetries rather than large strains and continuous broken symmetries.

Keywords: liquid crystal; elastomer; texture deformation; elasticity

1. Introduction

Liquid crystal elastomers are rubber-like solids that exhibit liquid crystal order. An elastomer (rubber) is a cross-linked polymer melt, which is to say it is made of long writhing entropically dominated polymer chains. After cross-linking the chains continue to behave as though they were still in a melt, but the presence of a few links between them prevents macroscopic flow so the material is a solid. The unwinding of these chains allows rubber to suffer very large ($\geq 100\%$) elastic strains recoverably and at modest energetic cost. A liquid crystal in contrast is a real fluid of rod-like molecules but with the solid-like property that the rods align, giving the fluid long-range orientational order. If liquid crystal rods are embedded inside an elastomer, either as constituents of the polymer chains or as pendent-like side chains, they can exploit the locally liquid-like nature of the elastomer network to align. This results in a liquid crystal phase trapped inside a solid rubber: a liquid crystal elastomer.

P.G. de Gennes' influence suffuses the study of liquid crystal elastomers. As well as significant contributions to the study of both liquid crystals (*1*) and polymers (*2*) he was also the first to think about combining them in elastomers. He first considered conventional elastomers cross-linked in the presence of liquid crystal solvents (*3*) and then later considered the coupling of nematic order and strain in cross-linked nematic polymer networks (*4*). The textured deformations reviewed in this article are a consequence of this coupling, so it is both fitting and a pleasure to dedicate it to him.

The study of textured deformations in liquid crystal elastomers was initiated by a beautifully simple experiment by Kundler and Finkelmann (*5*). They took a strip of nematic elastomer with a uniform in-plane nematic director and stretched it along the in-plane direction perpendicular to the original director. Their strip of elastomer did several remarkable things in response to being stretched. Before stretching the elastomer was homogenous and had no light scattering features so it was highly transparent, but on stretching it became completely opaque and remained opaque until some critical stretch $\lambda_e \approx 2$ was reached, at which point the elastomer sharply became transparent again. Furthermore, the strains up to λ_e were produced at very much lower stress than would have been expected for an elastomer without liquid-crystalline order, but the stresses required to produce further extension were not. Using optical microscopy and X-ray diffraction Kundler and Finkelmann were able to show that, as the sample was stretched, the liquid crystal director was rotating towards the stress direction. The cloudy phase consisted of many micrometre-scale stripes with alternating senses of director rotation as shown in Figures 1 and 2. These stripes provided the

*Email: jsb56@cam.ac.uk

ISSN 0267-8292 print/ISSN 1366-5855 online

DOI: 10.1080/02678290902879224
http://www.informaworld.com

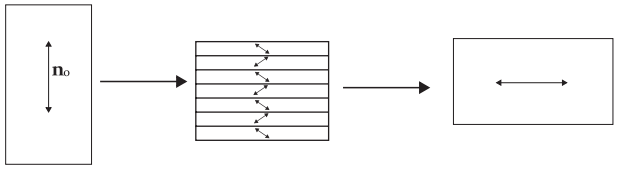

Figure 1. A strip of nematic elastomer with an initially homogenous in-plane director is stretched perpendicular to the director. It is first observed to form a cloudy phase consisting of stripes in which the director has rotated equal amounts but in opposite senses, then at some critical stretch rotation is completed and the elastomer becomes transparent again.

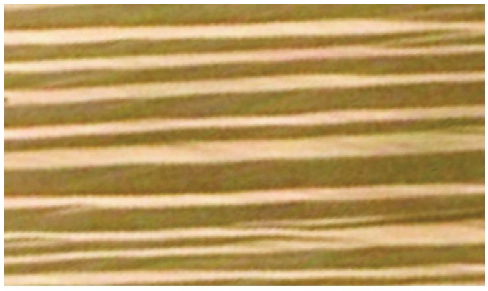

Figure 2. A view of the cloudy stripe phase through crossed-polars, the stripes of alternating director rotation are clearly visible. The length scale of the stripes is of the order of 10 μm (image by I. Kundler and H. Finkelmann).

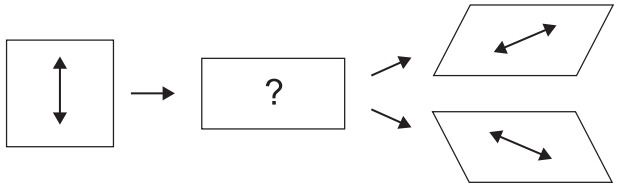

Figure 3. Left: A strip of relaxed nematic elastomer. Middle: Stretching the strip affinely perpendicular to its director is a high-energy deformation. Right: If the strip is allowed to shear as well as stretch the energy of the deformation is much reduced and the director rotates through the sample. The amount of shear required is zero at both the beginning and end of director rotation but finite at intermediate stages.

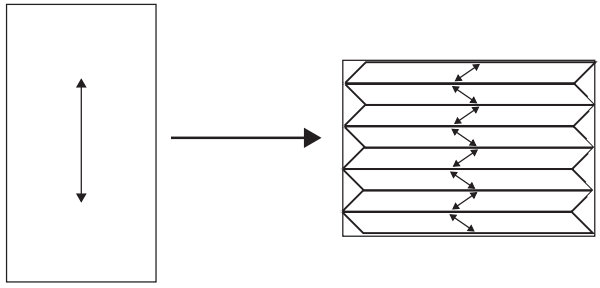

Figure 4. The energetic cost of a stretch perpendicular to the director is reduced by building the deformation out of stripes of low-energy sheared deformations: a texture. If the width of the stripes is very small the macroscopic deformation appears to be pure stretch.

heterogeneity to scatter light making the sample opaque, but when director rotation was complete the nematic director was again uniform so the sample returned to being transparent. The same results have been reproduced in (*6*) for a chemically very different nematic elastomer.

The surprising results of the Kundler and Finkelmann experiment are well explained by a textured deformation (*7*). The essential idea is that when the elastomer is stretched and the nematic director rotates, the energy of the deformation is much reduced if the elastomer also shears as shown in Figure 3. By splitting into many fine stripes that alternate between equal and opposite director rotation and shear, the elastomer is able to build the imposed deformation entirely out of low-energy sheared stripes: it has formed a texture, Figure 4. This analysis, along with a microscopic understanding of why the shear reduces the energy, was made by Verwey, Warner and Terentjev (*7*) (see also (*8*)). Since these early experiments a great deal of progress has been made in the theoretical description of these textured deformations, in particular by Conti, DeSimone, Dolzmann and Adams (*9–12*), and there are now several interesting textures which have been proposed theoretically but not yet observed. One of the key theoretical achievements is the discovery of the fully relaxed free energy for ideal nematic elastomers (*9*) as a function of imposed macroscopic deformation, that is, the energy after the adoption of the most favourable texture for the imposed deformation. In this review we outline the key theoretical ideas that underpin this progress and then review some of the interesting proposed textures and experimental geometries in which they might be observed. We illustrate the theoretical ideas using the example of ideal nematic elastomers to in effect re-prove the relaxation result in (*9*). We hope that the additional explanation in this review will make this proof more accessible to non-mathematicians.

The subjects of textured deformations and liquid crystal elastomers are covered in two excellent books (*13*) and (*14*). The former is a general text on all aspects of the physics of liquid crystal elastomers, while the latter is a study of textured deformations in a different system, solids showing martensitic transitions.

2. Basic elasticity

To study elasticity problems we must first consider a body in a reference configuration to deform. We define the region of space occupied by the body

in the reference configuration as Ω and label all of the points in the body by their position vectors $\mathbf{x}$. Any deformation of the body can be described by a vector function $\mathbf{x}'(\mathbf{x})$ that gives the new position vector of each point in the body. We can now characterise the local distortion of the body caused by the deformation by imagining embedding a small vector $\mathbf{R}$ between two points in the reference state and calculating what it becomes in the deformed state. If the vector spans between $\mathbf{x_1}$ and $\mathbf{x_2}$ in the reference state ($\mathbf{R} = \mathbf{x_1} - \mathbf{x_2}$) then in the deformed state it will be $\mathbf{R}' = \mathbf{x}'(\mathbf{x_1}) - \mathbf{x}'(\mathbf{x_2})$. Taylor expanding $\mathbf{x}'$ about $\mathbf{x}'(\mathbf{x_1})$ and keeping only the first-order term (because $\mathbf{x_2}$ is near $\mathbf{x_1}$) we see that $\mathbf{R}' = (d\mathbf{x}'/d\mathbf{x})\mathbf{R}$. We define this important first derivative that characterises the local distortion of the body as the deformation gradient $\underline{\underline{F}}(\mathbf{x}) = d\mathbf{x}'/d\mathbf{x}$. A deformation is called homogenous if $\underline{\underline{F}}$ is constant throughout the body. In this case there are no higher-order terms in the Taylor expansion of $\mathbf{x}'(\mathbf{x})$ so any vector $\mathbf{R}$ embedded between two points in the reference configuration will become $\underline{\underline{F}} \cdot \mathbf{R}$ in the deformed configuration. The transformation rule for vector areas is also important and is given by $\mathbf{A}' = (\mathrm{cof}\,\underline{\underline{F}})\mathbf{A}$, where $\mathbf{A}$ is the vector normal to a surface and with magnitude equal to the area of the surface. Since deformations in elastomers are always at constant volume (meaning $\det \underline{\underline{F}} = 1$; see the end of the section), this is the same as $\mathbf{A}' = \underline{\underline{F}}^{-\mathrm{T}}\mathbf{A}$ where the inverse transpose is represented by $-\mathrm{T}$.

The deformation gradient tensors for homogenous deformation are the same as the transformation matrices met in elementary mathematics: if the deformation was a rotation it is a rotation matrix, if it was a shear it is a shear matrix, etc. If a second deformation is applied to the deformed state the total deformation gradient is simply the matrix product of the two separate deformations. Elasticity in elastomers often involves very large deformations so, unlike in many other systems, these matrix products cannot be expanded and linearised about the identity matrix.

We can gain great insight into the nature of homogenous deformations by applying the polar decomposition theorem to the second rank tensor $\underline{\underline{F}}$. This tells us that we can always write $\underline{\underline{F}} = \underline{\underline{R}} \cdot \underline{\underline{S}}$ where $\underline{\underline{R}}$ is a rotation matrix, and $\underline{\underline{S}}$ is a symmetric matrix and, hence, in some frame diagonal. This means that any deformation can be thought of as a simple stretch, with three orthogonal principal axes, followed by a body rotation. Since only the former involves any distortion of the body, the amount of distortion is completely described by the three (positive) eigenvalues of $\underline{\underline{S}}$, $f_1 \leq f_2 \leq f_3$, which are called the principal values of the deformation $\underline{\underline{F}}$. The volume of the deformed body is simply the volume of the body in the reference state multiplied by $\det \underline{\underline{F}} = f_1 f_2 f_3$, which can easily be visualised by imagining a unit cube in the reference state whose edges align with the principal axes of $\underline{\underline{S}}$: after deformation the cube will be a cuboid with edges of length f_1, f_2 and f_3 so its total volume has increased by a factor of $\det \underline{\underline{F}}$.

3. Formulating texture problems

When a deformation is applied to a body we actually specify the configuration of the surface of the body, while the interior can relax to whatever configuration (consistent with the imposed surface configuration) has the lowest energy. Our intuition suggests that, if we have deformed the boundary homogeneously, we expect the interior to also undergo the same homogenous deformation. However, in textured deformations this is not the case. In these cases the energy of the interior is minimised by the body adopting a fine mixture of different deformations that are consistent with the deformed boundary. Our approach to understanding this type of problem is therefore one of energy minimisation. We expect textures to occur if they are energetically favoured. If we know the material's energy function, $W(\underline{\underline{F}})$, which tells us the energy cost of imposing a homogenous deformation gradient $\underline{\underline{F}}$, then we wish to study the problem

$$W^{\mathrm{r}}(\underline{\underline{F}}) = \min_{\mathbf{x}' = \underline{\underline{F}}\mathbf{x} \text{ on } \delta} \frac{1}{\mathrm{Vol}.\Omega} \int W(\nabla \mathbf{x}'(\mathbf{x}))\, d\mathbf{x}. \qquad (1)$$

By this definition, the relaxed energy function $W^{\mathrm{r}}(\underline{\underline{F}})$ is the average energy per unit volume of the body after the deformation gradient $\underline{\underline{F}}$ has been imposed on the boundary of the body and the body has adopted the most favourable (in general non-homogenous/textured) deformation $\mathbf{x}'(\mathbf{x})$ consistent with the imposed deformation of the boundary. A function is called quasiconvex if the formation of textured deformations does not lower the energy any further. By definition, relaxed energy functions are quasiconvex. Although the above definition of $W^{\mathrm{r}}(\underline{\underline{F}})$ appears to be dependent on the shape of the body, Ω, in fact it is not. Some fairly simple rescaling arguments can be used to show that if W relaxes to W^{r} in Ω it has the same relaxation for any shape of body (*14*).

4. Models of liquid crystal elastomers

The above formulation of textures as a consequence of energy minimisation makes it clear that textures must be a consequence of unusual forms for $W(\underline{\underline{F}})$. For a conventional elastomer (an ideal Gaussian rubber) the energy density after imposing a homogenous deformation gradient $\underline{\underline{F}}$ is, in suitable units (set so

$\frac{1}{2}\mu \equiv \frac{1}{2}k_bTn = 1$ where n is the number density of cross-links),

$$W(\underline{\underline{F}}) = \begin{cases} \mathrm{Tr}\ (\underline{\underline{F}} \cdot \underline{\underline{F}}^{\mathrm{T}}) = f_1^2 + f_2^2 + f_3^2 & \text{if } \det \underline{\underline{F}} = 1, \\ \infty & \text{otherwise.} \end{cases} \tag{2}$$

The extreme energy penalty for $\det \underline{\underline{F}} \neq 1$ requires that all deformations take place at constant volume. This is a very good approximation for all elastomers since their bulk modulus is several magnitudes larger than their shear modulus, in future expressions it will be assumed that $\det \underline{\underline{F}} = 1$ so the penalty case will be omitted. This simple expression has several noteworthy features. It is only a function of the principal values of $\underline{\underline{F}}$ so it is isotropic: it only depends on the magnitudes of the three principal stretches, not what direction they are applied in. It also has a global minimum at $f_1 = f_2 = f_3 = 1$, so the elastomer is relaxed in the reference configuration. Finally, the energy penalty for stretching is quadratic in the three principal stretches, even at very large strain. This final property is what makes it a perfect rubber; in practice, real elastomers deviate from this behaviour at very high strains.

A nematic elastomer in a high-temperature isotropic state behaves in the same way as a conventional elastomer. However, when it is cooled into the nematic phase, all of the liquid crystal rods align in one direction (for monodomain samples; polydomains are not discussed here) and the elastomer spontaneously elongates in the alignment direction (*15*). The degree of elongation depends on the exact nature of the elastomer but can be up to several hundred percent. The underlying physical mechanism is that the liquid crystal rods bias the polymer strands' conformation distributions along the nematic director. Ideally any direction could have been chosen for the new nematic director, so this extension could have appeared along any direction and there is a large set of equivalent low-energy states each with a different deformation with respect to the isotropic state (Figure 5). The locally liquid-like nature of elastomers means that the nematic director can rotate through the elastomer, so if a deformation is applied that deforms one low-energy elongated state into another, the director can rotate to the appropriate angle meaning the deformation has not cost any energy to impose. The idea of soft elastic modes as a consequence of symmetry breaking spontaneous distortions was first studied by Golubovic and Lubensky (*16*).

We include spontaneous elongation in the energy function of the elastomer by making a single simple modification to the conventional elastomer energy, writing

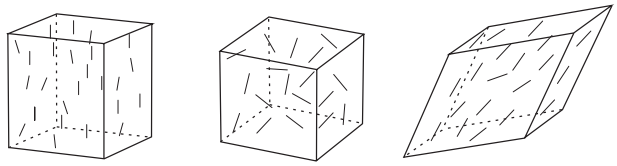

Figure 5. Middle: A cube of liquid crystal rubber in the high-temperature isotropic phase, the liquid crystal rods are shown as black lines. Left and right: On cooling to the nematic phase, the nematic order can form in any direction and the sample spontaneously stretches in this direction. There is a large set of equivalent relaxed states each with a different deformation with respect to the isotropic reference state.

$$W(\underline{\underline{F}}) = \begin{cases} f_1^2 + f_2^2 + f_3^2/r & \text{if } \det \underline{\underline{F}} = 1, \\ \infty & \text{otherwise,} \end{cases} \tag{3}$$

where r is a scalar constant of the material that is greater than one in the nematic phase. This form of the energy can be justified microscopically by considering Gaussian distributed polymers with second moments biased by the nematic director (*17*). This microscopic treatment actually yields a more general energy function,

$$W(\underline{\underline{F}}, \mathbf{n}) = \mathrm{Tr}\left(\underline{\underline{F}} \cdot \underline{\underline{F}}^{\mathrm{T}} \cdot \left(\underline{\underline{\delta}} + \left(\frac{1}{r} - 1\right)\mathbf{n} \otimes \mathbf{n}\right)\right), \tag{4}$$

where $\underline{\underline{\delta}}$ is the identity matrix and $\mathbf{n}$ is the final state nematic director. This form predicts the cost of independently applying a deformation gradient $\underline{\underline{F}}$ and causing the nematic director to align along $\mathbf{n}$, but for elastic experiments the nematic director is not under experimental control but rather is free to rotate to whatever direction minimises the elastic energy, so the observed energy function is

$$W(\underline{\underline{F}}) = \min_{\hat{\mathbf{n}}} \mathrm{Tr}\left(\underline{\underline{F}} \cdot \underline{\underline{F}}^{\mathrm{T}} \cdot \left(\underline{\underline{\delta}} + \left(\frac{1}{r} - 1\right)\mathbf{n} \otimes \mathbf{n}\right)\right), \tag{5}$$

which is minimised when $\mathbf{n}$ aligns with the axis of the largest principal value of $\underline{\underline{F}}$ returning equation (3). In other contexts $\mathbf{n}$ can be manipulated, for example by using electric fields (*18*) or light (*19*).

We can visualise the important difference between the nematic and conventional elastomer energies by plotting the energy cost of imposing a simple uniaxial stretch ($f_1 = f_2 = 1/\sqrt{f_3}$) in different directions (Figure 6). If $\boldsymbol{\rho}$ is a two-dimensional vector from the origin, these plots display the cost of imposing a uniaxial stretch along $\boldsymbol{\rho}$ with magnitude $f_3 = |\boldsymbol{\rho}| + 1$. The reference undeformed state is at the origin ($f_3 = f_2 = f_1 = 1$). The function for a

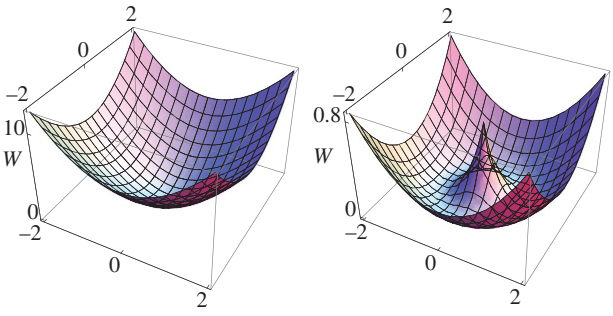

Figure 6. Energetic cost of imposing a uniaxial stretch on a conventional elastomer (left) and nematic elastomer (right) in the reference state. The value of the function at $\boldsymbol{\rho}$ is the cost of imposing a uniaxial stretch of magnitude $|\boldsymbol{\rho}|+1$ in the direction of $\boldsymbol{\rho}$.

conventional elastomer is convex with a global minimum at the undeformed state, but the function for a nematic elastomer is not convex and has a degenerate set of minima corresponding to relaxed states in a ring around the origin, while the reference state is not a relaxed state.

In this work we use the high-temperature isotropic state as the reference state from which deformations are measured. The advantage of this approach, introduced in (*9*) and familiar from the study or martensite, is clear: from this isotropic reference state the energy function (3) is isotropic, and therefore the energy function of the relaxed elastomer will also be isotropic. If the aligned nematic state is taken as the reference state the function is no longer isotropic because it can distinguish between stretches applied along and perpendicular to the nematic order. The price paid for this mathematical convenience is that the reference state is not a relaxed state but a high-energy state: the elastomer would like to stretch and form a nematic phase. Since real samples are well-aligned nematic monodomains the results must be translated into this more physical reference configuration to discuss experimental results. Historically much work has been done using the aligned nematic state as the reference state (*7, 8*), and the appropriate energy function for this case is (*13*)

$$W(\underline{\underline{F}}') = \min_{\hat{\mathbf{n}}} \mathrm{Tr}\left(\underline{\underline{F}}' \cdot (\underline{\underline{\delta}} + (r-1)\mathbf{n}_0 \otimes \mathbf{n}_0) \cdot \underline{\underline{F}}'^{\mathrm{T}} \cdot \left(\underline{\underline{\delta}} + \left(\frac{1}{r} - 1\right)\mathbf{n} \otimes \mathbf{n}\right)\right), \tag{6}$$

where $\mathbf{n}_0$ is the nematic director in the reference nematic state, $\mathbf{n}$ is the final director and $\underline{\underline{F}}'$ is now the deformation gradient from the reference nematic state. This form can be deduced from (5) by substituting $\underline{\underline{F}} = \underline{\underline{F}}' \cdot \underline{\underline{F}}_{\mathrm{S}}$ where $\underline{\underline{F}}_{\mathrm{S}}$ is a spontaneous deformation that results in nematic order along $\mathbf{n}$.

The formation of textured deformations is ultimately driven by energy functions such as (3), functions which assign little energetic cost to some large distortions and much higher cost to some smaller distortions. In the field of liquid crystal elastomers the large deformations at low energy are generated, as in the nematic case, by the rotation of the liquid crystal director through the elastomer causing a large change to the polymer conformations, and hence the shape of the sample, at modest energetic cost. The existence of these low-energy modes, which correspond to deformations that take the sample around the well in Figure 6, is well established. Two particularly compelling papers are (*8*), a treatment of the Kundler and Finkelmann experiment where both stripping and the exact nature of director rotation as a function of stretch are explained using soft elastic modes, and (*18*) where soft modes are seen as a response to director rotation caused by electric fields.

5. Geometric bound on the deformations made soft by texture

Since the ideal nematic energy (3) has a large set of relaxed states, there is scope for making states with other deformations with respect to the reference state relaxed if they can be made out of textures of relaxed states. We can place a simple (although, as we show later, in practice perfect) bound on the set of deformations that can be made relaxed through the formation of texture.

Volume conservation requires that $\det \underline{\underline{F}} = 1 = f_1 f_2 f_3$ so we can substitute $f_2 = 1/(f_1 f_3)$ into (3) giving

$$W(\underline{\underline{F}}) = f_1^2 + \frac{1}{f_1^2 f_3^2} + \frac{f_3^2}{r}. \tag{7}$$

Simple differentiation shows that this is minimised at $3r^{-1/3}$ by $f_3 = r^{1/3}$, $f_1 = f_2 = r^{-1/6}$, which correspond to the ring of minima in Figure 6. This means that any uniaxial stretch by a factor of $r^{1/3}$ will turn the reference state into a low-energy relaxed state, irrespective of the axis of the stretch. These are the spontaneous distortions of the system that are seen on cooling an isotropic sample to the nematic phase, seen, for example, in (*15*) and first predicted in (*20*). If we define K^0 as the set of minimisers of (7), then we can write

$$K^0 = \{\underline{\underline{F}} \in \mathbb{M}^{3\times 3} : f_1 = f_2 = 1/r^{1/6},\ f_3 = r^{1/3}\}. \tag{8}$$

(This set notation will be familiar to mathematicians. The curly brackets denote a set, $\in$ means 'is a member of', ':' means 'such that' and $\mathbb{M}^{3\times 3}$ is the set of 3×3 matrices, so this expression reads 'the set of 3×3

matrices $\underline{\underline{F}}$ such that the principal values of $\underline{\underline{F}}$ are $f_1 = f_2 = 1/r^{1/6}$ and $f_3 = r^{1/3}$'.) We can now put a simple bound on the set K^{qc}, the total set of deformations that, for ideal nematic elastomers, can be made relaxed by the formation of texture. If a texture is to be relaxed it must be made entirely out of deformations that are relaxed, i.e. members of K^0. If $\underline{\underline{F}}$ is a member of K^{qc}, it is built out of members of K^0, so it is clearly impossible for the largest principle value of $\underline{\underline{F}}$ to exceed $r^{1/3}$ as this would require $\underline{\underline{F}}$ to be a larger deformation than any of the deformations that make it up. Similarly, the smallest principal value cannot be smaller than $r^{-1/6}$, so we can write

$$K^{qc} \subseteq \{\underline{\underline{F}} \in \mathbb{M}^{3\times 3} : r^{-1/6} \leq f_1 \leq f_2 \leq f_3 \leq r^{1/3}\}, \quad (9)$$

where $\subseteq$ denotes that K^{qc} is either a subset of or equal to the set on the right. For example, in Figure 4, the imposed stretch deformation is in K^{qc} because it can be made out of a texture of two sheared deformations that are in K^0.

6. Continuity of textured deformations

To establish that a deformation $\underline{\underline{F}}$ is actually in K^{qc} we need to explicitly construct a texture of zero-energy deformations that averages to $\underline{\underline{F}}$. To do this, it is not enough to find a set of deformation gradients in K^0 that average to $\underline{\underline{F}}$ and then apply them to small regions of the body in the appropriate volume fractions. This is because two deformation gradients cannot in general be applied in adjacent regions without the boundary between the regions fracturing. For example, it is impossible to rotate one part of a body and not an adjacent part without the boundary between the two ripping. Textured deformations require the deformation gradient to become a function of position in the material, so different parts of the material deform differently. However, when choosing spatially changing deformation gradients, we must remember that $\underline{\underline{F}}(\mathbf{x}) = d\mathbf{x}'/d\mathbf{x}$ where $\mathbf{x}'(\mathbf{x})$ gives the position vectors after deformation of points in the material originally at $\mathbf{x}$. If the body is not to fracture, then $\mathbf{x}'(\mathbf{x})$ must be a smooth function which means that $\underline{\underline{F}}(\mathbf{x})$, as the gradient of a smooth function, must have zero curl.

The zero-curl condition is useful for situations where $\underline{\underline{F}}(\mathbf{x})$ is a smoothly varying function. However, textured deformations are almost never smooth but rather consist of many small regions each with a constant deformation gradient, and therefore have sharp changes in the gradient across the boundaries. Applying the condition that $\underline{\underline{F}}(\mathbf{x})$ has zero curl when it is piecewise constant is difficult. A simpler approach is to realise that two deformations, $\underline{\underline{F}}_1$ and $\underline{\underline{F}}_2$, applied on either side of a plane boundary will not cause the material to rip provided that the boundary plane deforms into the same plane under both deformations. If $\mathbf{m}$ is the boundary normal in the reference state, this requires that $\underline{\underline{F}}_1\mathbf{v} = \underline{\underline{F}}_2\mathbf{v}$ for every vector $\mathbf{v}$ perpendicular to $\mathbf{m}$, meaning every $\mathbf{v}$ in the interfacial plane in the reference state. This will be true if the deformation gradients are rank-one connected, meaning

$$\underline{\underline{F}}_1 - \underline{\underline{F}}_2 = \mathbf{a} \otimes \mathbf{m} \quad (10)$$

where $\mathbf{a}$ is any vector; we show below that $\mathbf{a}$ is actually always a vector in the interfacial plane in the final state. We can easily prove that this condition is sufficient to guarantee the material does not rip by contracting the equation with $\mathbf{v}$ giving

$$\underline{\underline{F}}_1\mathbf{v} - \underline{\underline{F}}_2\mathbf{v} = 0, \quad (11)$$

which is precisely the condition required for continuity.

The condition of rank-one connectivity is equivalent to requiring that vector areas in the interfacial plane transform to the same vector areas under both deformations (*14*),

$$\underline{\underline{F}}_1^{-\mathrm{T}}\mathbf{m} = \underline{\underline{F}}_2^{-\mathrm{T}}\mathbf{m} \equiv \mathbf{m}', \quad (12)$$

where we have defined $\mathbf{m}'$ as the final state boundary normal. Contracting the rank-one connectivity condition from the left with $\mathbf{m}' = \underline{\underline{F}}_1^{-\mathrm{T}}\mathbf{m} = \underline{\underline{F}}_2^{-\mathrm{T}}\mathbf{m}$ we see that $0 = (\mathbf{m}' \cdot \mathbf{a}) \otimes \mathbf{m}$. This means that $\mathbf{a}$ is perpendicular to the deformed state plane normal, $\mathbf{m}'$, and hence is a vector in the interfacial plane in the deformed state. The geometry of rank-one connected deformations is shown in Figure 7.

Rather more insight into the nature of the rank-one connectivity constraint is yielded by writing it as

$$\underline{\underline{F}}_1 = \left(\underline{\underline{\delta}} + \mathbf{a} \otimes \mathbf{m}'\right)\underline{\underline{F}}_2, \quad (13)$$

where $\underline{\underline{\delta}}$ is the identity matrix and, since $\mathbf{a}$ and $\mathbf{m}'$ are orthogonal, the tensor preceding $\underline{\underline{F}}_2$ on the right is a

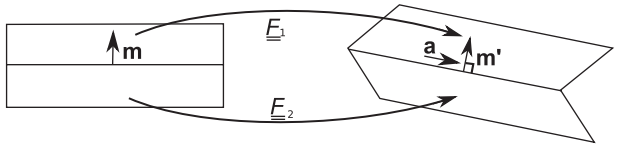

Figure 7. A body split into two regions by a plane with normal $\mathbf{m}$ undergoes different deformations $\underline{\underline{F}}_1$ and $\underline{\underline{F}}_2$ on either side of the boundary. The two deformations are rank-one connected ($\underline{\underline{F}}_1 - \underline{\underline{F}}_2 = \mathbf{a} \otimes \mathbf{m}$) so they do not cause the body to rip at the boundary.

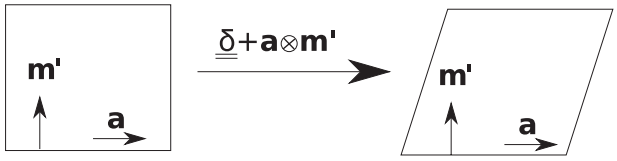

Figure 8. Two deformations that are rank-one compatible differ only by a final state simple shear across the final state boundary. The final state boundary normal is **m**′.

simple shear; see Figure 8. This means that the deformation on one side of the boundary relative to the other side of the boundary is just a simple shear across the boundary. It is easy to see that a simple shear across a boundary does not cause the material to fracture, as shown in the stripes of opposite shear in Figure 4.

The rank-one connectivity condition places a very strong constraint on which deformation gradients can be applied next to each other. Most pairs of deformation gradients are not rank-one connected, and even if two deformation gradients are rank-one connected there will only be one plane (with normal **m** in the reference state) across which they can join. This rules out most more complicated texture geometries such as those with curved boundaries.

7. Laminate textures

There is a simple way for a material to form a fine texture out of two deformation gradients that are rank-one connected: it can form a laminate. All of the planes that separate regions of different deformation must have the same layer normal (**m** in the reference configuration), and hence be parallel so by splitting into a stack of layers separated by such parallel planes the material can oscillate between the two deformation gradients on a fine scale, achieving their average macroscopically. The Kundler and Finkelman stripe domain, Figures 4 and 2, is an example of a laminate texture.

All of the textures that have been explicitly considered in the field of liquid crystal elastomers are laminates. The reason for this is that the number of different types of boundary increases rapidly with number of deformation gradients in a texture, so with two gradients there is only one type of boundary, but with three there are three types and with four there are six. Each type of boundary needs to be rank-one connected, so the number of continuity relations that must be satisfied also increases rapidly. Furthermore, the different types of boundaries will not be parallel so intersections between boundaries will need to be considered which have further continuity constraints (*14*). However, one trick which has been used to construct textures that involve more than two deformations in both SmC (*11*) and nematic (*9*) elastomers is higher-order lamination. This entails lamination between two deformation gradients that are rank-one connected and are themselves made relaxed by the formation of laminates, making a second-order lamination between two laminated deformations. This allows four deformation gradients to make up the final texture while only having three continuity equations (one for each simple lamination and one for the second-order lamination) and, by separation of length scales, being able to neglect the intersections between the different laminate interfaces.

8. Laminates in ideal nematic elastomers

8.1 Morphology of nematic stripe domains

The minimisers of (3) are any deformations with principle values $f_1 = f_2 = r^{-1/6}$ and $f_3 = r^{1/3}$, meaning any uniaxial stretch of magnitude $r^{1/3}$. Figure 9 shows two such stretches applied on either side of a plane boundary. It is clear that only if the boundary bisects the axes of the two stretches will it be stretched to the same degree along the boundary by both deformations. However, if the deformations are simple stretches then, although the boundary will be stretched to the same degree by both, it will be rotated differently and the body will still fracture. For the deformations to be rank-one continuous the stretches must be followed by body rotations that restore the continuity of the boundary. This simple construction shows that the nematic director, which aligns with the long axis of the stretch, must always form equal and opposite angles with the boundary normal on either side of the boundary, as was observed in the Kundler and Finkelman experiment (Figure 1). This simple result does not seem to have previously appeared in the liquid crystal elastomer literature. The results of the Kundler and Finkelman experiment can be neatly explained by considering the successive states given

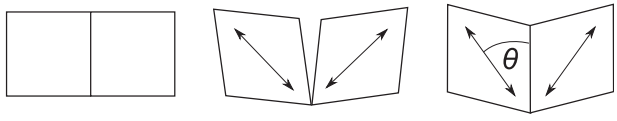

Figure 9. Left: A body in the reference configuration is split into two regions by a plane. Middle: Uniaxial stretches are applied to the two regions. They are not compatible so the sample rips along the boundary. The arrows indicate the axis of the stretch, and consequently the nematic director. Right: If the two regions are now rotated the boundary between them becomes continuous again. Many repetitions of this structure makes a stripe domain.

by this construction as θ moves from $\pi/2$ (the start of the experiment) to 0 (the end of the experiment).

This construction can be put on a more rigorous footing using two theorems originating in the study of solids showing martensitic transitions. These theorems are useful for establishing the morphology of textures. The first states that if $\underline{\underline{Q}}$ is a rotation matrix the equation

$$\underline{\underline{F}}_1 - \underline{\underline{Q}} \cdot \underline{\underline{F}}_2 = \mathbf{a} \otimes \mathbf{m} \tag{14}$$

has, for fixed $\underline{\underline{F}}_1$ and $\underline{\underline{F}}_2$, either two or zero solutions, which in general will have different $\underline{\underline{Q}}$, $\mathbf{a}$ and $\mathbf{m}$ (see (*21*)). The second, known as Mallard's law, states that if $\underline{\underline{F}}_1^{\mathrm{T}} \cdot \underline{\underline{F}}_1 = \underline{\underline{R}} \cdot \underline{\underline{F}}_2^{\mathrm{T}} \cdot \underline{\underline{F}}_2 \cdot \underline{\underline{R}}$ for some π rotation $\underline{\underline{R}}$ there are certainly two solutions, one of which has $\mathbf{m}$ along the axis of $\underline{\underline{R}}$ (see (*22*)). There are also simple forms for $\mathbf{m}$ for the second solution and for $\mathbf{a}$ for both solutions. More details can be found in (*14*). Taking $\underline{\underline{F}}_1$ and $\underline{\underline{F}}_2$ as two uniaxial stretches that minimise (3) with axes $\mathbf{n}_1$ and $\mathbf{n}_2$ (so $\underline{\underline{F}}_1 = r^{-1/6}(\underline{\underline{\delta}} + (\sqrt{r} - 1)\mathbf{n}_1 \otimes \mathbf{n}_1)$ and likewise for $\underline{\underline{F}}_2$) we see that Mallard's law is satisfied if the axis of $\underline{\underline{R}}$ is taken as either $\mathbf{n}_1 + \mathbf{n}_2$ or $\mathbf{n}_1 - \mathbf{n}_2$ so that $\underline{\underline{R}}\mathbf{n}_2 = \pm\mathbf{n}_1$. This means there are certainly two solutions to the continuity equation, one with $\mathbf{m} \propto \mathbf{n}_1 - \mathbf{n}_2$ and one with $\mathbf{m} \propto \mathbf{n}_1 + \mathbf{n}_2$. Therefore, any two minimisers of (3) can, after an appropriate body rotation, form a laminate texture, and that the boundary normal of the stripe domain must always bisect the nematic directors (which align with the stretch axes) on either side of the boundary. The first theorem then tells us that these are no more solutions to (14) with minimisers of (3) so there are no stripe domains between relaxed states that do not have this property.

8.2 The full set of low-energy textured deformations

We can use the idea of laminate textures to find the full set of deformations that can be achieved with the same energy as a relaxed monodomain by the formation of texture, K^{qc}. In the following section we explicitly construct textures (double and single laminates) that allow any deformation in the upper bound on K^{qc} in (9) to be achieved with this energy density. This is necessarily quite abstract, so less mathematically inclined readers may prefer to skip to Section 9 where the full relaxation result is stated and discussed.

Let K^1 be the set of deformations that can be made soft by forming laminate textures between two members of K^0. This means that if a deformation $\underline{\underline{F}}$ is in K^1 the elastomer can realise this deformation by splitting into a stack of layers with layer normal $\mathbf{m}$ and undergoing alternating soft deformations F^+ and F^- (both in K^0). For this to work $\underline{\underline{F}}^+$ and $\underline{\underline{F}}^-$ must be compatible (rank-one connected), meaning that for some $\mathbf{a}$,

$$\underline{\underline{F}}^+ - \underline{\underline{F}}^- = \mathbf{a} \otimes \mathbf{m}, \tag{15}$$

and the average deformation must be $\underline{\underline{F}}$, so, if the volume fractions of $\underline{\underline{F}}^+$ and $\underline{\underline{F}}^-$ are α and $1-\alpha$, respectively, $\alpha\underline{\underline{F}}^+ + (1-\alpha)\underline{\underline{F}}^- = \underline{\underline{F}}$. We can write this more compactly as

$$K^1 = \{\underline{\underline{F}} = \alpha\underline{\underline{F}}^+ + (1-\alpha)\underline{\underline{F}}^- : \underline{\underline{F}}^+, \underline{\underline{F}}^- \in K^0, \underline{\underline{F}}^+ - \underline{\underline{F}}^- = \mathbf{a} \otimes \mathbf{m}\}. \tag{16}$$

If $\underline{\underline{F}}$ is in K^1 and is made soft by lamination between $\underline{\underline{F}}^+$ and $\underline{\underline{F}}^-$ with texture normal $\mathbf{m}$, we know that, since two of the principal values of $\underline{\underline{F}}^+$ are $r^{-1/6}$, there is a whole plane of unit vectors such that $|\underline{\underline{F}}^+\hat{\mathbf{e}}| = r^{-1/6}$. This plane must intersect with the plane perpendicular to $\mathbf{m}$ with at least a line, let the vector $\mathbf{v}$ be a unit vector on this common line. Dotting the continuity equation (15) onto $\mathbf{v}$ we see that

$$\underline{\underline{F}}^+\mathbf{v} = \underline{\underline{F}}^-\mathbf{v}. \tag{17}$$

Therefore, $\underline{\underline{F}}\mathbf{v} = \underline{\underline{F}}^+\mathbf{v}$ and $|\underline{\underline{F}}\mathbf{v}| = r^{-1/6}$, so lamination between two soft deformations must produce an overall deformation $\underline{\underline{F}}$ with $f_1 = r^{-1/6}$, so

$$K^1 \subseteq \{\underline{\underline{F}} \in \mathbb{M}^{3\times3} : r^{-1/6} = f_1, \det(F) = 1\}. \tag{18}$$

Physically this simply means that in the direction perpendicular to both long stretches (into the page in Figure 9) the total stretch must be $r^{-1/6}$. We now construct single laminates to show that all deformations with this property can be constructed by the lamination of members of K^0.

The polar decomposition theorem tells us that any deformation can be fully characterised by three simple stretches in three orthogonal directions (by the three principal values of the deformation) followed by a body rotation. The latter cannot change the energy of the deformation, and since the reference state is isotropic (see (7)), nor can the choice of directions to impose the three perpendicular stretches. Therefore, we expect the energy of the deformation to be only a function of the principal values of the deformation.

According to (18) the most general set of principal values that might be compatible with being in K^1 are $f_1 = r^{-1/6}$, $f_2 = \mu_2$ and $f_3 = \mu_3$ where $r^{-1/6} \le \mu_2 \le \mu_3$ and $\mu_2\mu_3 r^{-1/6} = 1$ but μ_2 and μ_3 are otherwise

unconstrained. The simplest deformation with these principal values is the symmetric matrix with the principal values as its eigenvalues. If $\underline{\underline{F}}$ is this matrix, then in some frame it is diagonal giving $\underline{\underline{F}} = \mathrm{diag}(r^{-1/6}, \mu_2, \mu_3)$. If we take

$$\underline{\underline{F}}^{\pm} = \begin{pmatrix} r^{-1/6} & 0 & 0 \\ 0 & \mu_2 & \pm\delta \\ 0 & 0 & \mu_3 \end{pmatrix} \tag{19}$$

we see that $\underline{\underline{F}} = \frac{1}{2}\underline{\underline{F}}^{+} + \frac{1}{2}\underline{\underline{F}}^{-}$ and

$$\underline{\underline{F}}^{+} - \underline{\underline{F}}^{-} = 2\delta \mathbf{e}_2 \otimes \mathbf{e}_3, \tag{20}$$

so $\underline{\underline{F}}^{+}$ and $\underline{\underline{F}}^{-}$ are compatible and can form a laminate structure that averages to $\underline{\underline{F}}$. Therefore, if $\underline{\underline{F}}^{+}$ and $\underline{\underline{F}}^{-}$ are in K^0 (are soft deformations), then $\underline{\underline{F}}$ can be made into a soft deformation by adopting this texture, and is in K^1. One principal value of both $\underline{\underline{F}}^{+}$ and $\underline{\underline{F}}^{-}$ is $r^{-1/6}$ (by construction), the other two principal values are given by the square roots of the solutions of

$$\det\left[\begin{pmatrix} \mu_2 & \pm\delta \\ 0 & \mu_3 \end{pmatrix}\begin{pmatrix} \mu_2 & \pm\delta \\ 0 & \mu_3 \end{pmatrix}^{\mathrm{T}} - t\begin{pmatrix} 1 & 0 \\ 0 & 1 \end{pmatrix}\right] = 0. \tag{21}$$

The solutions of this characteristic equation, which are the same for both $\underline{\underline{F}}^{+}$ and $\underline{\underline{F}}^{-}$, are given by

$$t = \frac{1}{2}(\mu_2^2 + \mu_3^2 + \delta^2) \pm \sqrt{\frac{1}{2}(\mu_2^2 + \mu_3^2 + \delta^2)^2 - \mu_2^2\mu_3^2}. \tag{22}$$

This solution explains the placement of δ in (19): we can now tune its value to adjust the principal values of $\underline{\underline{F}}^{\pm}$ to ensure they are in K^0. It could not have been placed in either the top row or left-hand column without disrupting the smallest principal value, which we need to be $r^{-1/6}$, but it could equivalently have been placed in the diagonally opposite slot. For $\underline{\underline{F}}^{+}$ and $\underline{\underline{F}}^{-}$ to be soft deformations, their principle values must be $r^{-1/6}$, $r^{-1/6}$ and $r^{1/3}$, so the solutions of this equation must be $r^{-1/3}$ and $r^{2/3}$. These values for the solutions are obtained by taking

$$\delta = \frac{1}{r^{1/3}}\sqrt{r^{2/3} - \mu_2^2}\sqrt{r^{2/3} - \mu_3^2}. \tag{23}$$

Furthermore, we see that our existing conditions on μ_2 and μ_3 ($r^{-1/6} \le \mu_2 \le \mu_3$, $\mu_2\mu_3 r^{-1/6} = 1$) ensure that these square roots are always real, so for any μ_2 and μ_3 consistent with $\det(\underline{\underline{F}}) = 1$ and the smallest principle value of $\underline{\underline{F}}$ being $r^{-1/6}$ we can find a δ such that $\underline{\underline{F}}^{+}$ and $\underline{\underline{F}}^{-}$ are both soft deformations that can form a laminate structure averaging to $\underline{\underline{F}}$. Therefore, we have shown that every element in the set given in (18) is in K^1, so this upper bound on the set is in fact the exact result,

$$K^1 = \{F \in \mathbb{M}^{3\times3} : r^{-1/6} = f_1, \det(F) = 1\}. \tag{24}$$

The physical description of these single laminates is straightforward: they are just a general presentation of the 'stripe domains' that have already been predicted (*7*) and observed (*8*). They are simply stripes of alternating shear and director rotation with the directors and plane normal all being in a common plane, as sketched in Figure 4. All of the textures that have been constructed here have equal volume fractions of two deformations in K^0. Clearly laminate structures with different volume fractions can be made, but this cannot include any more deformations in K^1 only provide alternate laminate textures for deformations that are already in K^1.

8.2.1 Second-order laminates

We have found the set of all deformations that can be made soft by simple laminate textures, K^1, but this is somewhat smaller than the upper bound for the full set of soft deformations given in (9). This suggests we should look at laminates within laminates, meaning laminates formed by alternating layers each of which have undergone a deformation in K^1 that is itself soft by virtue of lamination. Let the set of all soft deformations that require second rank lamination be called K^2,

$$\{K^2 = \{\underline{\underline{F}} = \alpha\underline{\underline{F}}^{+} + (1-\alpha)\underline{\underline{F}}^{-} : \underline{\underline{F}}^{+}, \underline{\underline{F}}^{-} \in K^1, \underline{\underline{F}}^{+} - \underline{\underline{F}}^{-} = \mathbf{a} \otimes \mathbf{m}\}. \tag{25}$$

As in the single laminate case, we expect membership of K^2 to only depend on a deformations principle values. Taking the simplest possible matrix with principal values $\mu_1 \le \mu_2 \le \mu_3$ (where $\mu_1\mu_2\mu_3 = 1$), $\underline{\underline{F}} = \mathrm{diag}(\mu_1, \mu_2, \mu_3)$, we see that

$$\underline{\underline{F}}^{\pm} = \begin{pmatrix} \mu_1 & 0 & \pm\delta \\ 0 & \mu_2 & 0 \\ 0 & 0 & \mu_3 \end{pmatrix} \tag{26}$$

are again compatible deformations that average to $\underline{\underline{F}}$, so if we can find a δ such that $\underline{\underline{F}}^{\pm}$ are in K^1, $\underline{\underline{F}}$ is indeed

in K^2. One principal value of $\underline{\underline{F}}^{\pm}$ is clearly μ_2, the other two are given by the square roots of the solutions to the equation

$$\det\left[\begin{pmatrix}\mu_1 & \pm\delta\\ 0 & \mu_3\end{pmatrix}\begin{pmatrix}\mu_1 & \pm\delta\\ 0 & \mu_3\end{pmatrix}^{\mathrm{T}}-t\begin{pmatrix}1 & 0\\ 0 & 1\end{pmatrix}\right]=0. \quad (27)$$

which is familiar from the previous section. Its solutions are

$$t=\frac{1}{2}(\mu_1^2+\mu_3^2+\delta^2) \pm\sqrt{\frac{1}{2}(\mu_1^2+\mu_3^2+\delta^2)^2-\mu_1^2\mu_3^2}. \quad (28)$$

For $\underline{\underline{F}}^{\pm}$ to be in K^1, we require that their smallest principle value be $r^{-1/6}$, so the smaller root of this equation must be $r^{-1/3}$. This is true if we choose

$$\delta=r^{1/6}\sqrt{\mu_1^2-r^{-1/3}}\sqrt{\mu_3^2-r^{-1/3}}. \quad (29)$$

Since, by definition, $\mu_1\le\mu_2\le\mu_3$ this choice of δ is real provided that $\mu_1\ge r^{-1/6}$. Clearly any $\underline{\underline{F}}$ with $r^{-1/6}\le\mu_1\le\mu_3\le r^{1/3}$ satisfies this condition, moreover, since the requirement $\det(F)=1$ implies $\mu_1\mu_2\mu_3=1$, we cannot find any $\underline{\underline{F}}$ with $r^{-1/6}\le\mu_1$ but $\mu_3\ge r^{1/3}$. The principle values of $\underline{\underline{F}}$ are simply μ_1, μ_2 and μ_3 so we see that

$$K^2\supseteq\{\underline{\underline{F}}\in\mathbb{M}^{3\times3}: r^{-1/6}\le f_1\le f_3\le r^{1/3}\}. \quad (30)$$

However, this is precisely the same set as the upper bound on K^{qc} given in (9). Since K^{qc} is the set of all deformations that can be made soft by adopting microstructure, it must be bigger than or equal to K^2. Therefore, the only possibility is that both sets and the bound are all equal, that is

$$K^2=K^{\mathrm{qc}}=\{F\in\mathbb{M}^{3\times3}: r^{-1/6}\le f_1\le f_3\le r^{1/3}\}. \quad (31)$$

From this we conclude that the set of all fully relaxed deformations can be made relaxed by first- or second-order lamination, so there is no need to consider higher-order laminates.

The physical interpretation of double laminates is a little harder than the single laminates. They can be thought of as the result of taking a single laminate structure and trying to stretch it perpendicular to the laminate normal and the liquid crystal directors (which are all in a plane). Deformations of this type clearly have the potential to be soft because the director starts perpendicular to the stretch direction so it can rotate towards it. However, as the director rotates, as well as stretching the sample in the required direction, shear also builds up. It is this shear that is eliminated by the second-order lamination, which is between regions of opposite director rotation and opposite shear.

8.3 Laminates that cost energy

By inspecting K^{qc} we see that if a deformation $\underline{\underline{F}}$ is not soft, it must have its smallest principal value $f_1<r^{-1/6}$ (despite $\det\underline{\underline{F}}=1$ this does not require $f_3>r^{1/3}$, for example $f_1=r^{-2/3}$, $f_2=f_3=r^{1/3}$ is not in K^{qc}). This means that if it is built out of a texture, at least some of the deformations that make up the texture must also have smallest principal values less than $r^{-1/6}$. The energy of a monodomain that has deformed without texture is

$$W=f_1^2+\frac{1}{f_1^2f_3^2}+\frac{f_3^2}{r}. \quad (32)$$

If we fix f_1 and minimise over f_3 we see that the lowest-energy deformation consistent with this choice of f_1 is given by

$$f_3=\frac{r^{1/4}}{\sqrt{f_1}}, \quad (33)$$

which implies

$$f_2=\frac{1}{f_1f_3}=\frac{1}{r^{1/4}\sqrt{f_1}}. \quad (34)$$

This is a highly anisotropic deformation with $f_3/f_2=\sqrt{r}$, which is that same high anisotropy as deformations in K^0. If we apply a deformation with this f_1 that is more anisotropic in f_2 and f_3 there is no scope for using textures to lower the energy, so the sample will just deform as a monodomain with the energy given by (32). Let the set of such deformations be S, where

$$S=\left\{\underline{\underline{F}}\in\mathbb{M}^{3\times3}:\frac{f_3}{f_2}\ge\sqrt{r},\det\underline{\underline{F}}=1\right\}. \quad (35)$$

This leaves the set

$$I=\left\{\underline{\underline{F}}\in\mathbb{M}^{3\times3}:\frac{f_3}{f_2}<\sqrt{r},f_1<\frac{1}{r^{1/6}}\det\underline{\underline{F}}=1\right\} \quad (36)$$

unaccounted for. These are deformations with f_2 and f_3 less anisotropic than is energetically desirable, so they can lower their energy by splitting into textures where each region is made out of more anisotropic (and

hence lower energy) deformations. This sounds like it could become very complicated, but in fact the result is fairly simple: if you fix f_1, any deformation with $f_3/f_2 < \sqrt{r}$ can be achieved by a single laminate structure built out of deformations which have the same value for f_1 but with the optimal values for f_2 and f_3, namely $f_3/f_2 = \sqrt{r}$. Such a structure has energy

$$W = f_1^2 + \frac{1}{f_1^2 f_3^2} + \frac{f_3^2}{r} \tag{37}$$

$$= \frac{2}{\sqrt{r} f_1} + f_1^2. \tag{38}$$

Showing that this optimal energy can be achieved could be done straightforwardly by again using the constructions in the preceding sections to find the laminates that can form between domains with fixed f_1 and $f_3/f_2 < \sqrt{r}$. However, it is more instructive to consider these deformations as derived from compressions of K^1. Deformations in K^1 also have $f_3/f_2 < \sqrt{r}$ because this is enforced by the condition $f_1 = r^{-1/6}$. Therefore, every deformation in I can be thought of as a deformation in K^1 with principal values $f_1 = r^{-1/6}, f_2$ and f_3 that has been followed by a uniaxial compression along the direction of f_1 by γ to give a new deformation with principal values $r^{-1/6}/\gamma$, $\sqrt{\gamma} f_2$ and $\sqrt{\gamma} f_3$. Any deformation in I can be constructed in this way. However, the deformations in K^1 were constructed out of laminates of deformations with principle values $r^{-1/6}$, $r^{-1/6}$ and $r^{1/3}$, so when we compress the structure to obtain the deformation in I it is still a laminate structure but built out of deformations with principle values $r^{-1/6}/\gamma$, $\sqrt{\gamma} r^{-1/6}$ and $\sqrt{\gamma} r^{1/3}$. These still have $f_3/f_2 = \sqrt{r}$ so they are precisely the optimal laminate structures that were claimed to exist in the previous paragraph.

9. Relaxed energy functions

We are now in a position to write out the full relaxed energy function for ideal nematic elastomers,

$$W^{\mathrm{qc}}(F) = \begin{cases} 3r^{-1/3} & \text{if } F \in \mathrm{K}^{\mathrm{qc}} \\ 2/(r^{1/2} f_1) + f_1^2 & \text{if } F \in I \\ f_1^2 + f_2^2 + f_3^2/r & \text{if } F \in S \\ \infty & \text{otherwise} \end{cases} \tag{39}$$

where

$$I = \left\{ \underline{\underline{F}} \in \mathbb{M}^{3\times 3} : \tfrac{f_3}{f_2} < \sqrt{r}, f_1 < \tfrac{1}{r^{1/6}}, \det \underline{\underline{F}} = 1 \right\}$$

$$S = \left\{ \underline{\underline{F}} \in \mathbb{M}^{3\times 3} : \tfrac{f_3}{f_2} \geq \sqrt{r}, \det \underline{\underline{F}} = 1 \right\}$$

$$K^{\mathrm{qc}} = \{ \underline{\underline{F}} \in \mathbb{M}^{3\times 3} : r^{-1/6} \leq f_1 \leq f_3 \leq r^{1/3}, \det \underline{\underline{F}} = 1 \}.$$

The 'otherwise' case only contains deformations with $\det \underline{\underline{F}} \neq 1$ that do not conserve volume.

However, whilst the arguments in the preceding sections demonstrate that textures exist that allow the elastomer to relax to this energy, the arguments that this is the furthest it can relax have not been at all rigorous. This poses a general question: how do we know when an energy function is relaxed and no longer susceptible to the formation of further textures?

When a material is deformed, it will respond with a textured deformation if there is a texture of deformations such that the average of the energy of the deformations is lower than the energy of the average of the deformations. This suggests the underlying cause of the formation of textures is a lack of convexity in the energy function. This suggestion is backed up by the plots of the energy functions for nematic and conventional elastomers (Figure 6) which show that the nematic energy is much less convex than the conventional energy. Reassuringly, if we plot the same graph for our relaxed nematic energy function it is now convex (Figure 10).

In one dimension the lack of simple convexity is indeed the cause of textured deformations. Consider a long rod that is stretched (affinely) by a factor of λ at an energetic cost of $W(\lambda)$. It will be energetically favourable for the rod to split into length fractions f and $(1-f)$ which undergo stretches λ_1 and λ_2, respectively, if $f\lambda_1 + (1-f)\lambda_2 = \lambda$, so the average stretch matches that imposed, and $fW(\lambda_1) + (1-f)W(\lambda_2) \leq W(\lambda)$ which is precisely the condition that W be a non-convex function. If we plot $W(\lambda)$ and draw a straight line between $W(\lambda_1)$ and $W(\lambda_2)$, a point on the line a fraction f of the distance between the two points gives the average energy and stretch of a texture consisting of a fraction f of the material undergoing λ_1 and a fraction $(1-f)$ of the material undergoing λ_2. If the point lies above

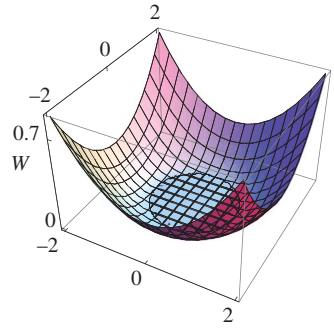

Figure 10. Energetic cost of imposing a uniaxial stretch on a nematic elastomer in the reference state after formation of the optimal texture; compare with Figure 6. The flat disc at the middle of the plot is a set of deformations made completely relaxed by texture formation.

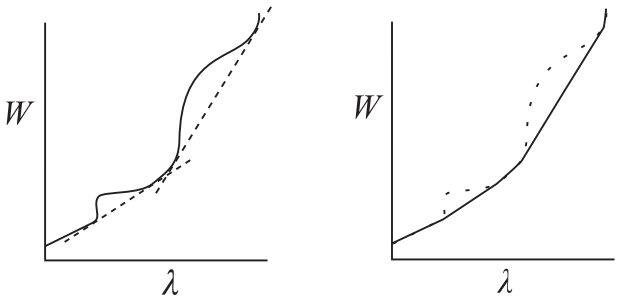

Figure 11. Left: A non-convex one-dimensional energy function $W(\lambda)$, the dotted lines are tangent to points on the curve on either side of the regions of non-convexity. Right: Texture formation allows the energy function to relax to its convex envelope, which falls on the common tangents sketched on the left over intervals in which the original function was non-convex.

the curve, the texture does not save energy, but if it lies below it does. The relaxed energy function is thus simply the convex envelope of $W(\lambda)$, meaning the highest valued convex function that is nowhere larger than $W(\lambda)$. An example of this construction is shown in Figure 11. This can be constructed using the 'common tangent' construction where regions of non- convexity are replaced by the straight line which is tangent to the curve on both sides of the region.

In higher dimensions the notion of convexity is not as helpful in making progress because W is a function of the deformation gradient $\underline{\underline{F}}$ not the scalar stretch λ. The problem is that convexity is not compatible with the principle of frame indifference, which states that simply rotating the final state after deformation should not cost any energy. Consider the deformation gradients $\underline{\underline{F}}_1 = \mathrm{diag}(1,1,1)$ and $\underline{\underline{F}}_2 = \mathrm{diag}(1,-1,-1)$. The first is simply identity, which is to say it does not deform at all, while the second is a π rotation about some axis. The principle of frame indifference dictates that both these deformations must cost the same amount of energy since they are only different by a final state body rotation. If $W(\underline{\underline{F}})$ was genuinely convex then $\underline{\underline{F}}_3 = \frac{1}{2}\underline{\underline{F}}_1 + \frac{1}{2}\underline{\underline{F}}_2 = \mathrm{diag}(1,0,0)$ would also have to cost the same energy, despite the fact that it has a determinant of zero and collapses a three-dimensional solid body onto a line. This does not matter because it is impossible to build a texture out of $\underline{\underline{F}}_1$ and $\underline{\underline{F}}_2$ without ripping the body, so although the energy function is not convex between $\underline{\underline{F}}_1$ and $\underline{\underline{F}}_2$ we cannot build textures that exploit this lack of convexity. However, if $\underline{\underline{F}}_1$ and $\underline{\underline{F}}_2$ had been rank-one connected and hence able to form laminate textures, we would be able to form textures that exploited the lack of convexity. This means that relaxed energy functions need to be rank-one convex (*23*), meaning that $W^{\mathrm{r}}(\underline{\underline{F}} + \gamma \mathbf{a} \otimes \mathbf{n})$ is a convex function of γ for any $\underline{\underline{F}}$, $\mathbf{a}$ and $\mathbf{n}$.

A rank-one convex energy function is not susceptible to the formation of laminate textures. However, such a function may be subject to the formation of other more exotic textures. The true defining feature of a relaxed function is that it is quasiconvex, meaning

$$W^{\mathrm{qc}}(\underline{\underline{F}}) = \min_{\mathbf{x}'=\underline{\underline{F}}\mathbf{x} \text{ on } \delta} \frac{1}{\mathrm{Vol.}\Omega} \int W^{\mathrm{qc}}(\nabla \mathbf{x}'(\mathbf{x}))\, d\mathbf{x}, \quad (40)$$

which simply states that a function is quasiconvex if its energy cannot be lowered by texture formation, so the minimum over all possible textured deformations consistent with imposing $\underline{\underline{F}}$ on the boundary (right-hand side) is simply the same as the energetic cost of imposing $\underline{\underline{F}}$ homogeneously throughout the body (left-hand side). However, proving quasiconvexivity directly is usually very difficult. In the case of ideal nematic elastomers we can proceed using an important theorem proved by Ball (*24*). We say that a scalar function $W^{\mathrm{pc}}(\underline{\underline{F}})$ is polyconvex if there is a another function g with two matrix arguments $\underline{\underline{A}}$ and $\underline{\underline{B}}$ and a scalar argument c such that $g(\underline{\underline{A}}, \underline{\underline{B}}, c)$ is convex in $\underline{\underline{A}}$, $\underline{\underline{B}}$ and c and has the property that if you replace $\underline{\underline{A}}$ with $\underline{\underline{F}}$, $\underline{\underline{B}}$ with $\underline{\underline{F}}^{-T}$ and c with $\det \underline{\underline{F}}$ you obtain $W^{\mathrm{pc}}(\underline{\underline{F}})$. Ball's theorem says that a polyconvex function is quasiconvex and, hence, fully relaxed and not susceptible to further formation of texture (*24*), although the reverse is not true, and the physical meaning of polyconvexity is unknown.

To show that the proposed form (39) is polyconvex, we write it as a function of $\alpha = 1/f_1$ and $\beta = f_3$ (using $\det F = 1$) and then differentiate each part of the result, $\psi(\alpha, \beta)$, twice to show that it is a continuous, non-decreasing and convex function of both variables. This is a tedious exercise so it is not reproduced here. We then write $\alpha = \max_{\hat{\mathbf{e}}} |\underline{\underline{A}}\hat{\mathbf{e}}|$ and $\beta = \max_{\hat{\mathbf{e}}} |\underline{\underline{B}}\hat{\mathbf{e}}|$. These are convex functions of $\underline{\underline{A}}$ and $\underline{\underline{B}}$, respectively, because the maximum of a sum is always less than or equal to the sum of the maxima. The function $g(\underline{\underline{A}}, \underline{\underline{B}}) = \psi(\max_{\hat{\mathbf{e}}} |\underline{\underline{A}}\hat{\mathbf{e}}|, \max_{\hat{\mathbf{e}}} |\underline{\underline{B}}\hat{\mathbf{e}}|)$ is therefore a convex function of $\underline{\underline{A}}$ and $\underline{\underline{B}}$ because a convex non-decreasing function of a convex function is always a convex function. Finally, since $g(\underline{\underline{F}}, \underline{\underline{F}}^{-T}) = W^{\mathrm{qc}}(\underline{\underline{F}})$, we conclude that W^{qc} is polyconvex and hence relaxed.

10. Physical interpretation of W^{qc}

The physical interpretation of W^{qc} is clouded by the fact that it is written in terms of deformations from a high-energy reference state whereas in practice one normally thinks of deformations from a well-aligned

relaxed state. However, to reach the four different regimes from an aligned state is straightforward. If you stretch perpendicular to the director we enter K^1 and the elastomer forms zero-energy, planar single laminates. This is the Kundler and Finkelmann geometry (*8*). If you take such a sample already showing laminates and stretch it in the third direction (i.e.perpendicular to the original director and the original stretch) it enters K^2 and forms zero-energy, double-laminate textures. If instead of stretching a laminate sample you compress it in this third direction it will enter the I regime of energy-costing single laminates. Finally if you take an aligned monodomain and stretch it along its director you will enter S, the regime of hard elasticity without texture or director rotation.

If the result for W^{qc} is taken literally, the elastomer can be regarded as being liquid like when it is in K^{qc} since, at the set's interior, which is K^2, all deformations in the vicinity of the current deformation are soft so the elastomer should be able to flow. In contrast, in the S regime the elastomer is definitely behaving as a conventional elastic solid, with greater deformations costing more energy. In the I regime, behaviour is intermediate since the deformations do cost energy but the energy only depends on the smallest principal value of the deformation. In the plane perpendicular to this direction the elastomer is still behaving like a fluid. However, these classifications neglect both the semi-soft nature of real elastomers and the interfacial energies of texture planes which, in particular, will mean the zero-energy set of deformations is not actually zero energy, so the elastomer will not truly flow.

11. Length-scale of textures

In all of the above work, we have implicitly assumed that the laminate textures are formed on an infinitely small length scale. In practice, in the Kundler and Finkelmann experiment the laminates formed with widths between 1 and 100 μm (Figure 2). This length scale can be understood as the result of a competition between the interfacial energy of the laminate boundaries and the energy cost to the material of not quite meeting the imposed deformation at the boundary. A full analysis of this competition can be found in (*8*), here we simply give an overview of the source of the interfacial energy.

To model the interfacial energy we need two new physical ideas. The first is the Frank energy, familiar from conventional liquid crystals, which is an energy penalty for gradients (curves) in the nematic director. Second, the energy function (7) was developed under the assumption that the nematic director always aligns with the axis of most stretch from the isotropic state. This is certainly the conformation that minimises the elastic energy, but in situations where there are other processes that couple to the director (such as the Frank energy) it is possible for the nematic director to rotate away from this direction. The full model in (*17*) (equation (4)) includes this possibility and predicts a large elastic cost for this type of director rotation. At the boundary between laminates these two ideas conflict because the nematic director must bend sharply at the boundary. If the bend is very sharp it carries a high Frank energy, but if it is not sharp there is a large region in the middle of the boundary where the nematic director is rotated away from its preferred orientation. The competition between these two effects determines both the width and the interfacial cost of the boundary. A dimensional analysis suggests (correctly) that the appropriate characteristic width is $\sqrt{K/\mu} \sim 10^{-8}$m, where K is the Frank coefficient (in the one constant approximation) and $\mu = k_b Tn$, where n is the number density of cross-links, is the shear modulus of the nematic elastomer. This is much less than the characteristic stripe width of around 10^{-5} m, so the picture of stripes of completely homogenous deformations with very thin interfaces between them is accurate.

12. The effect of non-ideality

In reality nematic elastomers are not ideal, rather the nematic director has a slight preference to align in a certain direction and deformations that cause the director to rotate away from this preferred direction are not truly soft but rather cost a little energy. We can write down an expression for this non-ideal nematic energy that incorporates this idea,

$$W(\underline{\underline{F}}) = f_1^2 + f_2^2 + \frac{f_3^2}{r} - \beta|\underline{\underline{F}}\mathbf{n}_0|^2, \qquad (41)$$

where $\mathbf{n}_0$ is the preferred direction. This energy was originally derived microscopically in (*25*). Unfortunately, the full relaxed form of this energy has not been found, although it has been solved for thin films in extension (*10*). From the perspective of texture, the addition of non-ideality has two consequences. First, it breaks the large degeneracy of the ideal system: it assigns slightly different energies to different textures that previously produced the same macroscopic deformation at the same energy cost. For example, all of the textures that have been explicitly constructed in the ideal nematic case are laminates involving equal volume fractions of two different energy gradients; however, once two deformation gradients have been found to be rank-one compatible, and hence can laminate, they can do so with any volume fraction, meaning that the laminate textures

in K^1 can, in fact, be realised in many different ways. The construction shows that all deformations in K^1 can be achieved by simple lamination of two soft deformation gradients, and that no other deformation gradients can be made soft in this way, but it does not help to determine which lamination will take place. Non-ideality breaks this degeneracy and helps determine which textures will actually occur. In particular, one of the main results of (*10*) is that laminations which have their layer normal along $\mathbf{n}_0$ (in the reference configuration) are preferred, and often will not have equal volume fractions.

The second important consequence of non-ideality is that deformations in the neighbourhood of the relaxed (nematic and aligned) state do not texture until they reach a (small) threshold magnitude. This was observed in the original Kundler and Finkelmann experiment and analysed in (*8*). The nature of the onset of rotation has also been analysed in (*26*). This second effect can be understood qualitatively as a consequence of the energy now having a unique global minimum at the relaxed state of the elastomer. Around this minimum the form of the energy is the same as that of a simple uniaxial solid, which is to say it is locally convex enough to stop textures forming between different deformations in the neighbourhood, and there is no incentive to form textures with deformations that lie outside the neighbourhood because they are far from the global minimum and hence higher in energy. Textures only form for deformations that are far enough away from the global minimum that there are other deformations even further away that are lower in energy.

13. Smectic elastomers

13.1 SmA elastomers

The underlying energy function for SmA elastomers has two key differences from the nematic energy function. First, SmA liquid crystals are layered, and the layers move affinely under deformation. Second, the liquid crystal phase has a strong energetic preference for remaining in the SmA state, so there is a large energy penalty associated with causing the director to deviate from the smectic layer normal or changing the inter-layer spacing (*27*). This means that SmA elastomers only have one relaxed state: the cross-linking state which has both the preferred layer spacing and the director aligned along the layer normal. However, this energy function is still susceptible to the formation of texture (*27, 28*). In this case the lack of convexity underlying the texture formation is caused by the large discrepancy between the high energetic cost of deformations that change the layer spacing and the much lower cost of those that do not. Figure 12 shows an example in which an average deformation of stretch along the layer normal is constructed out of two low-energy in-plane shears. This is completely analogous to the 'Helfrich–Hurault' effect in liquid SmA systems first described in (*29*).

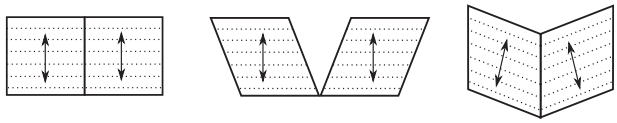

Figure 12. Texture formation in a SmA elastomer. The smectic layers are shown as dotted lines, and the director, which is always perpendicular to the layers, is shown as a double-headed arrow. By splitting into two regions that first shear then body rotate the average deformation is a simple stretch along the layer normal, but the inter-layer spacing has not changed.

The full form of the relaxed energy for a simplified SmA-type energy function is presented in (*28*), the proof proceeds in an analogous way to the analysis of the ideal nematic system and depends on the construction of double-laminate structures. Stretching experiments have been conducted on SmA elastomers, including along their layer normal (*30, 31*). In these experiment the elastomer deformed affinely at small stretches but with a complex texture at large stretches, which is the behaviour predicted by the model in (*28*). The instability to texture formation in this geometry was first analysed in (*27*).

13.2 SmC elastomers

SmC elastomers can be modelled using exactly the same energy as nematic elastomers but with the additional assumption that the smectic layers deform affinely and additional energy penalties for deformations that change the layer spacing or cause the director to rotate away from its preferred angle with the layer normal (*32*). In this approximation there is still a large set of relaxed states associated with the director occupying different directions in a cone around the layer normal. This set of relaxed states is essentially the subset of relaxed states for an ideal nematic elastomer that are consistent with the extra SmC constraints. The full set of deformations made relaxed by textures of relaxed states has been found (*11*) in a manner analogous to the ideal nematic case reviewed previously, although in this case not only double but triple laminates were required to complete the construction.

The description of simple laminates in SmC elastomers is more subtle than in nematics because the layers also form part of the morphology. Since the relaxed states of SmC elastomers are simply a subset

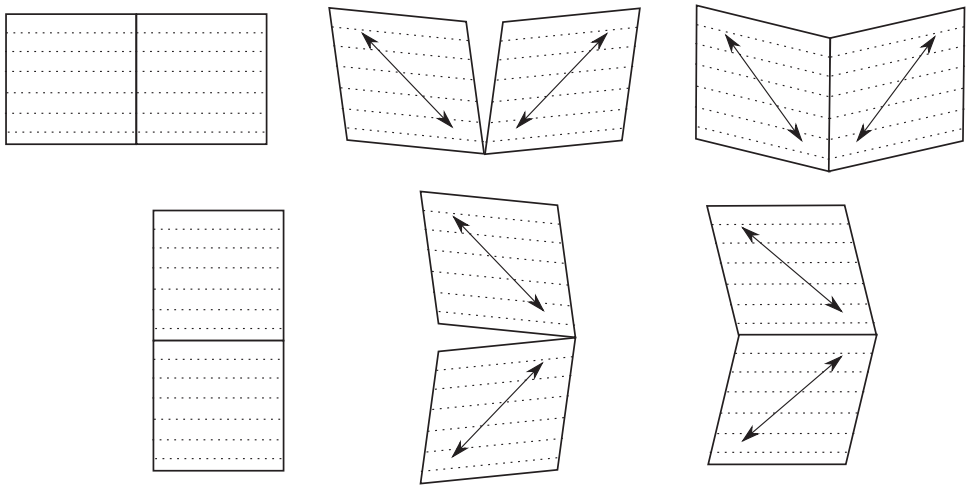

Figure 13. A construction analogous to Figure 5 but for SmC elastomers. As in the nematic case, the boundary normal must bisect the liquid crystal director for the deformations to be compatible. The smectic layers are shown as dotted lines, importantly the smectic layer normal may have a component out of the page although the boundary normal does not. The liquid crystal directors must also form equal angles with the dotted lines so that both the directors form the same angle with the smectic layer normal. For the elastomer to be in a relaxed state this must be the preferred tilt angle. These constraints permit two different morphologies: the first, shown in the top, in which the smectic layers are bent at the boundary, and the second, shown below, where they are not.

of those of nematic elastomers the stripe domains all have the same essential character as the nematic elastomers (discussed in Section 8.1), namely that the laminate boundary normal bisects the two directors. However, in addition to this basic property, the types of laminates that can form fall into two categories: one in which the smectic layers pass through the texture boundary apparently undeformed (*33*) and one in which the smectic layers are bent at the laminate boundary and the laminate boundary bisects the layer planes on either side of it (*34*). A construction illustrating these two basic types of boundary is shown in Figure 13.

14. Conclusions and interesting experiments

The theoretical study of textures in liquid crystal elastomers has made significant progress in the last 10 years. A very fruitful approach has been to start with an underlying material energy function $W(\underline{\underline{F}})$, usually inspired by statistical mechanics, and then prove that this relaxes by texture formation to a lower energy function $W^{\mathrm{r}}(\underline{\underline{F}})$. This is done by explicitly constructing laminate textures that allow the relaxation to happen, then showing that $W^{\mathrm{r}}(\underline{\underline{F}})$ is a quasiconvex function and hence there can be no further relaxation. In some cases, notably ideal nematic elastomers (*9*) and one model of SmA elastomers (*28*), this procedure is complete, while for other systems (ideal SmC and non-ideal nematic elastomers) only part of the solution is known, which is to say there are some deformations for which relaxing textures are known to exist and others for which there are no definitive conclusions. This approach allows us to pinpoint deformations that can be applied to elastomers which should lead to texture formation. However, it is not very good at predicting exactly which textures will occur because the very high symmetry of the material energy functions used means there are typically many textures which allow a given deformation to relax to its optimal energy. There is also no good scheme for enumerating all textures that allow a given deformation to relax to its optimal energy.

There are three ways of making concrete predictions about which textures will form. The first is to study their morphology (as in Section 8.1), which allows us to predict that in all nematic and SmC laminates between relaxed configurations the laminate normal will bisect the two liquid crystal directors, as they do in the Kundler and Finkelmann experiment. The second is to introduce non-ideality (semi-softness) into the model which breaks much of the degeneracy, but then the lower symmetry makes finding the relaxed energy function very difficult, and to date has only been done for thin nematics films in extension (*10*). The third approach is simply to rule categories of textures out. This is seen in the double-laminate case for ideal elastomers where the full set of deformations that can be made soft by single laminations is known, K^1, and it is smaller than the corresponding set for double

lamination, $K^2 = K^{qc}$. This means that for deformations in K^2 but not in K^1 textures are expected and single-laminate textures can be ruled out.

The lack of certainty over which textures will form makes experimental results particularly interesting. Not only will more observations test the theoretical predictions, but the observation of more textures may help the construction of a theory which makes clearer predictions about which textures will be observed. To this end, this review is concluded with a list of four experimental geometries that are predicted to produce interesting textured deformations.

14.1 Double laminates

The calculation of the full relaxed energy for ideal nematic elastomers contains a large set of deformations which can be made completely relaxed by the construction of double-laminate textures. These are textures in which two simple laminations, each of alternating stripes of two different deformation gradients, are then themselves laminated. These textures require the emergence of two length scales, the first lamination length scale between the individual deformations, and then a second much longer lamination length scale for the laminations between laminations. They are predicted to occur for deformations in which the elastomer is stretched in both directions perpendicular to the original director. This is a hard deformation to impose because the elastomers are in practice always thin films, and these deformations would require the thin film to be stretched in its thin direction. One way to achieve this would be to heat a nematic monodomain to the isotropic state, then cool it under the constraint that it cannot change shape perhaps by gluing it between glass slides of fixed separation. This enforces the deformation $\underline{\underline{F}} = \underline{\underline{\delta}}$ which is a deformation which can be made relaxed by the formation of double laminates, but not by the formation of single laminates.

The exact nature of the theoretical prediction in this case is not that double laminates will certainly form, but simply that something interesting must happen. The double-lamination construction proves that there are low-energy textures that the elastomer can adopt in this circumstance, and proves that they are not single laminates. We therefore expect the elastomer to adopt some texture which is approximately zero energy, which may or may not be double laminates, but must certainly be a type of texture that has not been observed before. Clarity as to what textures are observed may well accelerate and motivate further theoretical enquiry into this interesting question.

14.2 Single laminates always initially perpendicular to $\mathbf{n}_0$

The work by Conti *et al.* (*10*) on non-ideal nematic elastomers makes firmer predictions about which specific single-laminate structures will form than can be done with ideal nematic elastomers because the semi-softness breaks the large degeneracy of equal energy single laminates in the ideal system. It is predicted that the laminations that really occur will be those with boundary normals (in the initial state) parallel to the initial director. This leads to two new effects, first the texture normal will in some circumstances rotate with increased deformation, and second the stripe domains with non-equal volume fractions will be observed. The rotation of the laminate normals is simply caused by the rotation of the plane that is initially perpendicular to the initial director as a consequence of the macroscopic deformation.

One geometry in which both of these effects could be seen is simply stretching an aligned monodomain sample at an angle to the initial director. For texture to be observed the angle between the stretch axis and the initial director must be more than $\pi/4$ or the macroscopic deformation will stretch the direction corresponding to the initial director and no texture will be observed. The optimal angle is around $3\pi/8$ ($\theta = \pi/8$ in Figure 14) so that the geometry is neither too near the original Kundler–Finkelman experiment nor unable to show texture. The results in (*10*) predict that texture should form with equal volume fractions and boundary normals along the initial director, and then as stretching increases the volume fraction of the back-rotated species should reduce and that of the forward rotated species should increase until, at some critical stretch, only the latter remains and a monodomain is returned and subsequent deformation is hard. This is shown in Figure 14. These predictions are in contrast to those in (*7*) which predicts a different texture with laminate normals always perpendicular to the strain direction. This

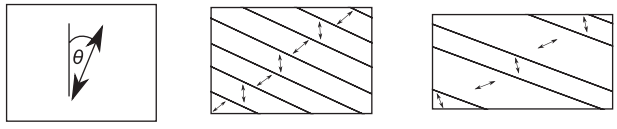

Figure 14. Experiment to confirm the preference for forming laminates with boundary normals perpendicular to the initial director. A relaxed sample is prepared and stretched at an angle θ to the relaxed director. At small stretches (but after a threshold) laminates appear with equal volume fractions of both senses of rotation. As stretching proceeds the volume fraction of back rotated stripes declines to zero and the texture returns to being a monodomain. The boundary planes rotate with increasing stretch as though they are embedded in the sample.

discrepancy is because, although the textures in (*7*) are relaxed textures for ideal nematic elastomers, they are not optimal for non-ideal specimens.

14.3 Novel lamination structures in SmC elastomers

Experimental geometries for observing texture in SmC elastomers are discussed at length in (*11*) and (*33*). The two most promising geometries are to shear a SmC elastomer as shown in Figure 15(a) (*33*) and to stretch at an angle to both the layer normal and director as shown in Figure 15(b) (see (*11*)). Both of these experiments have some technical difficulties, the shearing experiment because shearing a thin film without wrinkling is difficult, and the tensile experiment because there is only predicted to be a small set of axes (approximately $\pi/4 - \theta \leq \phi \leq \pi/4$) that will cause texture. A simpler experiment would be to shear in a slab geometry but in this case although textures have been predicted (also in (*33*)), they are not truly soft.

One of the textures proposed in the shearing geometry is particularly interesting. In (*33*), Warner and Adams propose a lamination in which the smectic layer plane does not change and the elastomer splits into equal volume fractions in which the liquid crystal director has rotated by equal amounts but in opposite senses around the smectic layer normal. As shearing proceeds the degree of rotation increases until both species have rotated by π and a monodomain is restored. If the layer normal is $(0, 0, 1)$ and the initial relaxed director is $(\sin\theta, 0, \cos\theta)$ (so θ is the relaxed director tilt angle), then, after some shear causing the director to rotate by $\pm\phi$, the two rotated directors will be $(\sin\theta\cos\phi, \pm\sin\theta\sin\phi, \cos\theta)$. Using the rule that the laminate normals must bisect the directors, this means the laminate normal must either be $(\sin\theta\cos\phi, 0, \cos\theta)$ or $(0, 1, 0)$. The latter is unlikely since it requires the lamination plane to be in the film. However, the first possibility is both reasonable and extremely interesting. It predicts that as shearing proceeds the laminates will rotate through the sample, starting perpendicular to the initial director and finishing perpendicular to the final director. This raises interesting questions about the motion of the laminate planes through the elastomer. It also predicts rotation of the director out of the plane of the film. Excitingly, it seems likely that this texture will be the texture favoured by the addition of semi-soft contributions to the model since it has continuous director rotation from the preferred direction and laminates initially perpendicular to the initial director.

There remains much ambiguity in predicting explicit textures in SmC elastomers, not least because there has been no study of semi-soft SmC systems analogous to (*10*), however these systems promise a rich set of textured responses. Work in this area is further motivated by the existence of chiral SmC* elastomers which show electrical polarisation along the cross product of the layer normal and liquid crystal director, making SmC* elastomers ferro-electric rubbers. This adds extra interest to the study of textured deformations since, if the polarisation vector cuts the laminate normals, they may become charged.

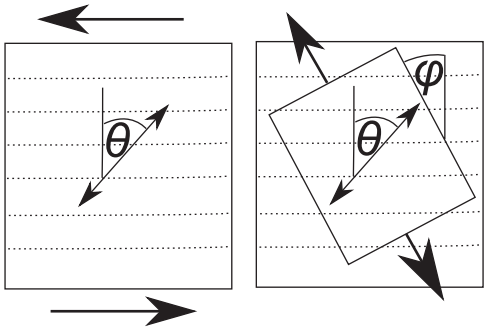

Figure 15. Experiments to induce textured deformations in SmC elastomers. The smectic layers are shown as dotted lines and the liquid crystal director as a double-headed arrow making an angle θ with the layer normal. Left: Shearing the elastomer as proposed in (*33*). This geometry should produce textures until the angle of the smectic director has been reversed, although wrinkling may be a problem. Right: Stretching the elastomer at an angle ϕ to the layer normal as discussed in (*11*). This stretch can be achieved by cutting a rectangle out of a film as indicated then stretching the new rectangular sample between clamps. Texture will only be observed for a very restricted set of choices of ϕ.

References

(1) de Gennes, P.G.; Prost, J. *The Physics of Liquid Crystals*, second edition; Oxford University Press: New York, 1995.
(2) de Gennes, P.G. *Scaling Concepts in Polymer Physics*; Cornell University Press: New York, 1980.
(3) de Gennes, P.G. *Phys. Lett. A* **1969**, *28*, 725.
(4) de Gennes, P.G. *C. R. Acad. Sci. B* **1975**, *281*, 101.
(5) Kundler, I.; Finkelmann, H. *Macromol. Chem. Rapid Comm.* **1995**, *16*, 679.
(6) Zubarev, E.; Kuptsov, S.; Yuranova, T.; Talroze, R.; Finkelmann, H. *Liquid Crystals* **1999**, *26* (10), 1531–1540.
(7) Verwey, G.C.; Warner, M.; Terentjev, E.M. *J. Phys. II France* **1996**, *6*, 1273–1290.
(8) Finkelmann, H.; Kundler, I.; Terentjev, E.M.; et al. *J. Phys. II* **1997**, *7*, 1059.
(9) DeSimone, A.; Dolzmann, G. *Arch. Rational Mech. Anal.* **2002**, *161*, 181.
(10) Conti, S.; DeSimone, A.; Dolzmann, G. *Phys. Rev. E* **2002**, *66*, 061710.
(11) Adams, J.M.; Conti, S.; DeSimone, A. *J. Cont. Mech. Ther.* **2006**, *18*, 319–334.

(12) Conti, S.; DeSimone, A.; Dolzmann, G. *J. Mech. Phys. Solids* **2002**, *50*, 1431–1451.
(13) Warner, M.; Terentjev, E.M. *Liquid Crystal Elastomers*, second edition; Oxford University Press: Oxford, 2007.
(14) Bhattacharya, K. *Microstructure of Martensite*; Oxford University Press: Oxford, 2003.
(15) Clarke, S.M.; Hotta, A.; Tajbakhsh, A.R.; Terentjev, E.M. *Phys. Rev. E* **2001**, *64*, 061702.
(16) Golubovic, L.; Lubensky, T. *Phys. Rev. Lett.* **1989**, *63*, 1082.
(17) Warner, M.; Bladon, P.; Terentjev, E.M. *J. Phys. II (France)* **1994**, *4*, 93.
(18) Urayama, K.; Honda, S.; Takigawa, T. *Macromolecules* **2006**, *39*, 1943–1949.
(19) Corbett, D.; Warner, M. *Phys. Rev. Lett.* **2007**, *99*, 174302.
(20) Warner, M.; Gelling, K.; Vilgis, T. *J. Chem. Phys.* **1988**, *88*, 4008.
(21) Ball, J.M.; James, R.D. *Arch. Rational Mech. Anal.* **1987**, *100*, 13–52.
(22) Ericksen, J.L. *J. Therm. Stres*. **1981**, *4*, 107–119.
(23) Conti, S. *J. Math. Pures Appl.* **2008**, *90*, 15–30.
(24) Ball, J.M. *Arch. Rational Mech. Anal.* **1976**, *63*, 337.
(25) Verwey, G.C.; Warner, M. *Macromolecules* **1995**, *28*, 4303–4306.
(26) Biggins, J.S.; Terentjev, E.M.; Warner, M. *Phys. Rev. E* **1994**, *78*, 041704.
(27) Adams, J.M.; Warner, M. *Phys. Rev. E* **2005**, *71*, 021708.
(28) Adams, J.M.; Conti, S.; DeSimone, A.; Dolzmann, G.; Dal Maso, G. *Math. Models Methods Appl. Sci.* **2008**, *18*, 1–20.
(29) Clark, N.A.; Meyer, R.B. *Appl. Phys. Lett.* **1973**, *22*, 493.
(30) Nishikawa, E.; Finkelmann, H. *Macromol. Chem. Phys.* **1999**, *200*, 312–322.
(31) Nishikawa, E.; Finkelmann, H.; Brand, H.R. *Macromolecular rapid communications* **1997**, *18*, 65–71.
(32) Adams, J.M.; Warner, M. *Phys. Rev. E* **2005**, *72*, 011703.
(33) Adams, J.M.; Warner, M. *Phys. Rev. E* **2008**, submitted.
(34) Biggins, J.S.; Bhattacharya, K. *Phys. Rev. E* **2008**, submitted.